Impurity transport in Alcator C-Mod in the presence of poloidal density variation induced by ion cyclotron resonance heating

A. Mollén[1], I. Pusztai[1,2], M. L. Reinke[2,3], Ye. O. Kazakov[4], N. T. Howard[2], T. Fülöp[1]

[1] *Department of Applied Physics, Chalmers University of Technology, Göteborg, Sweden*

[2] *Plasma Science and Fusion Center, Massachusetts Institute of Technology, Cambridge MA, USA*

[3] *University of York, Heslington, York, United Kingdom*

[4] *Laboratory for Plasma Physics, LPP-ERM/KMS, TEC Partner, Brussels, Belgium*

Introduction In the present work we study molybdenum transport in an ICRF heated Alcator C-Mod discharge [1], using local gyrokinetic simulations and theoretical modeling [2, 3] including the effect of poloidal asymmetries and plasma elongation. The predictions of molybdenum peaking from the modeling is compared to values from reconstruction of experimental measurements.

Experimental discharge We will examine the $1.0-1.2\,\mathrm{s}$ time slice of the Alcator C-Mod discharge 1120913016 with $3\,\mathrm{MW}$ hydrogen minority ICRH applied on the low-field-side. The ICRH resonant layer is tangential to the flux surface at $r/a=0.38$, where r is the minor radius and a the outermost minor radius. Molybdenum is an intrinsic impurity in Alcator C-Mod as the main material of the first wall. To constrain impurity diffusivity it is also introduced using a multi-pulse laser blow-off system in this discharge and its dynamics is tracked by multiple radiation imaging diagnostics [1]. The sawtooth inversion radius of the plasma is located in the region $0.32<r/a<0.40$, and an analysis of the SXR spectrograms indicates that no other MHD activity is present. We assume $n_z/n_e=5\times10^{-4}$, where the exact concentration is not critical as long as impurities are non-diluting trace, $Zn_z/n_e\ll1$. We assume a charge state Mo^{+32}; one of the dominant charge states around mid-radius. Impurity measurements are taken during the flat-top phases of the studied discharge, more than 200 ms after the ICRH has been switched on. The molybdenum density profiles are reconstructed from crystal spectroscopy data and we assume that the molybdenum temperature is equal to the main ion temperature.

The hydrogen minority fraction is almost constant at $f_H\equiv n_{H0}/n_{e0}=0.05$ throughout the analyzed radial domain, where the index '0' refers to the flux-surface averaged density. The on-axis toroidal magnetic field is $B_0=5.83\,\mathrm{T}$. The normalized resonant magnetic field strength is estimated as $B_c/B_0\approx0.89$, with B_c being the ICRH resonant magnetic field. Further details on the discharge are found in Ref. [4].

We will focus on the radial domain $r/a=0.20$–0.60, since this is a region where the ICRH has a considerable impact on the minority temperature anisotropy $\alpha_T\equiv T_\perp/T_\parallel$. Here, $T_\perp$ and $T_\parallel$ are

the perpendicular and parallel temperatures of the minority species. Within this radial domain the electron-ion collision frequency varies between $\nu_{ei} = 0.02$–$0.05\ c_s/a$, with $c_s = (T_e/m_i)^{1/2}$ being the ion sound speed. In our simulations collisions are modeled by the Lorentz operator. Furthermore, the effective normalized electron pressure is low, $\beta_e = 0.002$–0.005, justifying an electrostatic treatment. The moderate plasma rotation is neglected in our analysis. In particular we will calculate the molybdenum peaking with theoretical modeling for two radial locations: $r/a = 0.38$ tangential to the ICRH resonance and $r/a = 0.56$ intersecting the ICRH resonance.

Fluxes and mode characteristics The characteristics of the turbulence present in the studied discharge is analyzed with GYRO [5], neglecting the poloidal asymmetries arising from the ICRH. The main plasma species remain almost unaffected by the poloidal asymmetries, only impurities are affected due to their high charge, and since the impurities are in trace quantities they have a small impact on the turbulence. The Miller model equilibrium is used in our simulations, with $\mathcal{O}(\epsilon)$ corrections to the drift frequencies retained.

Nonlinear GYRO simulations show that the main part of the fluxes are ITG driven in around $k_y\rho_s = 0.40$ at both radial locations. The simulated electron energy fluxes conform with experiments within uncertainties within ± 10 % variations of a/L_{Ti}. The turbulent ion energy fluxes from GYRO are significantly higher than the experimental fluxes when only a trace Mo is included, however they are sensitive to small changes in local plasma parameters, especially a/L_{Ti}. Using a more realistic ion composition of B^{+5}, Ar^{+18} and Mo^{+32} in contents of $n_\mathrm{B}/n_e = 0.02$, $n_\mathrm{Ar}/n_e = 10^{-3}$ and $n_\mathrm{Mo}/n_e = 2\times10^{-4}$, resulting in a plasma effective charge of $Z_\mathrm{eff} = 1.90$, reduces the GYRO ion energy fluxes significantly closer to the experimental values. Performing a full sensitivity study to different plasma parameters, it is reasonable to believe that the ion energy fluxes can be matched within their experimental uncertainty. However it seems unlikely that both Q_i and Q_e could be matched simultaneously without a multi-scale GYRO analysis.

The largest Mo^{+32} fluxes are also driven at $k_y\rho_s = 0.40$. Comparing the turbulent Mo^{+32} fluxes from GYRO to neoclassical Mo^{+32} fluxes from NEO [6] simulations we find that $\Gamma^\mathrm{GYRO}_\mathrm{Mo}/\Gamma^\mathrm{NEO}_\mathrm{Mo} \gtrsim 10$. The NEO simulations are performed taking into account both plasma rotation and temperature anisotropy from ICRH. The size of the neoclassical fluxes is sensitive to plasma rotation, but remains an order of magnitude smaller than the size of the turbulent fluxes.

Molybdenum density peaking The effect of ICRH on the poloidal minority ion distribution was discussed in Refs. [2, 7, 8], and in Ref. [9] it was described how this could generate a poloidal variation in the non-fluctuating potential ϕ_E over a flux surface. The effect of the varying potential on turbulent impurity transport has been studied in Refs. [3, 9, 10] among others,

but limited to the situation when the studied flux surface does not intersect the ICRH resonance. In the present work the model for the potential is also based on Ref. [2], but we allow the flux surface to intersect the ICRH resonance keeping a more general situation. Figure 1 (a) shows the non-fluctuating potential from the model at the two studied radial locations, which leads to a displacement of the impurity distribution towards the inboard side of the flux surface. Figure 1 (b) shows the impurity density asymmetry strength. The dash-dotted line shows the numerically computed asymmetry of the single charge state of Mo^{+32}, considering only the effect from the minority density variation on the flux surface from ICRH and assuming $Z_{\mathrm{eff}} = 1.8$. The discrepancy between model and experiment is reduced when rotation effects are retained (dotted line). The remaining disagreement might be due to uncertainties in impurity content and rotation speed (suggesting that either or both of these may be higher than their nominal values).

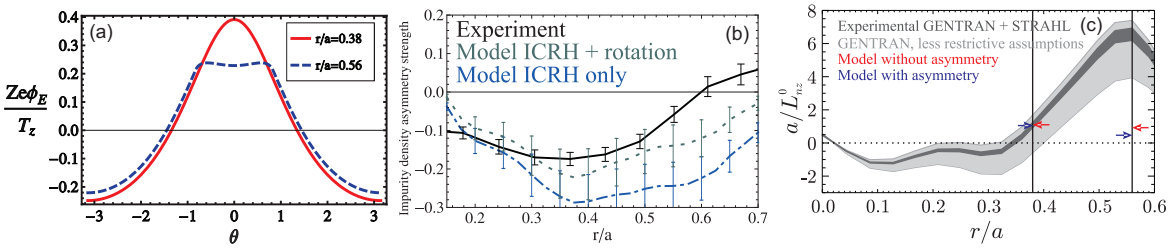

Figure 1: (a) Non-fluctuating potential as function of poloidal angle at $r/a = 0.38$ (solid) and $r/a = 0.56$ (dashed). (b) Comparison of the experimentally observed (solid) and numerically computed poloidal asymmetry due to ICRH only (dash-dotted) and with rotation retained (dotted). (c) Radial variation of the Mo^{+32} peaking factor. Light and dark gray shaded areas represent the experimental values calculated using a less and a more restricting set of assumptions on the uncertainties. Vertical bars mark the two studied radii. Arrows represent the theoretical estimates for the peaking factor at these radial locations; from the left (blue arrows): with asymmetries, from the right (red arrows): without asymmetries.

To study Mo^{+32} peaking we use the model of Ref. [3]. However, here we use an extended analysis by allowing the flux surface to intersect the ICRH resonance and retaining plasma elongation, κ. We assume a low-beta plasma and large-aspect-ratio, and neglect rotation and electrostatic trapping. The poloidally varying electrostatic potential is assumed to satisfy $Ze\phi_E/T_z \sim \mathcal{O}(1)$ (valid for the studied discharge as seen in Fig. 1 (a)), and since $Z \gg 1$ this implies that $e\phi_E/T_z \ll 1$. The potential gives rise to an $\mathbf{E}\times\mathbf{B}$ drift frequency $\omega_E = -\frac{k_y}{B}\frac{s\theta}{r\kappa}\frac{\partial\phi_E}{\partial\theta}$ in the linear gyrokinetic equation for the impurities. The equation is solved perturbatively in the small parameter $Z^{-1/2} \ll 1$, and the zero-flux impurity density gradient a/L^0_{nz} (peaking factor) is found from $\langle\Gamma_z\rangle = 0$ where $\langle\ldots\rangle$ denotes flux surface average. From linear GYRO simulations ϕ and ω are known. Further details on the model are found in Refs. [3, 4].

To calculate Mo^{+32} peaking we consider a single representative linear mode, $k_y\rho_s = 0.40$.

Figure 1 (c) shows the peaking factor at $r/a = 0.38$ and $r/a = 0.56$, when ϕ_E is excluded (red arrows) and included (blue arrows) in the model. The result is practically unaffected by the inclusion of the potential at $r/a = 0.38$, while at $r/a = 0.56$ it is decreased from $a/L^0_{nz} = 0.93$ to $a/L^0_{nz} = 0.49$. One of the reasons for the weak effect at $r/a = 0.38$ is a moderate value of the magnetic shear $s = 0.33$, at $r/a = 0.56$ the magnetic shear is $s = 0.78$ and the $\mathbf{E}_\theta \times \mathbf{B}_\varphi$-drift is stronger. $\mathcal{O}(\epsilon)$ corrections are also found to be relevant when determining the size of the effect.

Figure 1 (c) also shows experimental profiles (with uncertainties) of the Mo^{+32} peaking factor from the measured emission data. The profiles are constrained using the codes GENTRAN and STRAHL, details on the method are found in Ref. [1]. At $r/a = 0.38$, the calculated peaking factors fall within the more restrictive experimental range. However, the ones calculated for $r/a = 0.56$ strongly underestimate the experimental Mo^{+32} peaking factor.

Discussion and conclusions Comparing the linear gyrokinetic model for Mo^{+32} peaking to experimental measurements, we find agreement in the inner core at $r/a = 0.38$ but a strong discrepancy in the outer core at $r/a = 0.56$. The peaking is determined by some mechanism not included in our model at the outer location. Centrifugal and Coriolis drift effects (and the impact of rotation shear) have been neglected, but estimated to be small for the case we study. To obtain such a large peaking factor as seen experimentally for $r/a = 0.56$, there should be a drift frequency in the gyrokinetic equation several times larger than the diamagnetic drift frequency. Pure neoclassical transport could generate such a large peaking, but simulations show that neoclassical fluxes are an order of magnitude smaller than the turbulent. The radially increasing importance of atomic physics processes, such as the neutral fraction (which is not a measured quantity) and ionization/recombination of the studied single charge state, could play a role in the explanation. Another possibility would be that the discrepancy is due to a sawtooth effect, but the inversion radius of the studied discharge is well within $r/a = 0.56$.

[1] M. L. Reinke, N. T. Howard, et al, 55th Annual Meeting of the APS Division of Plasma Physics, Denver CO, USA, TP8.00037.
[2] Ye. O. Kazakov, I. Pusztai, et al, *Plasma Phys. Control. Fusion* **54**, 105010 (2012).
[3] I. Pusztai, A. Mollén, et al, *Plasma Phys. Control. Fusion* **55**, 074012 (2013).
[4] A. Mollén, I. Pusztai, et al, *Impurity transport in Alcator C-Mod in the presence of poloidal density variation induced by ion cyclotron resonance heating*, arXiv:1402.0309 (2014).
[5] J. Candy and R. E. Waltz, *J. Comput. Phys.* **186**, 545 (2003).
[6] E. A. Belli and J. Candy, *Plasma Phys. Control. Fusion* **50**, 095010 (2008).
[7] M. L. Reinke, I. H. Hutchinson, et al, *Plasma Phys. Control. Fusion* **54**, 045004 (2012).
[8] R. Bilato, O. Maj, et al, *Nucl. Fusion* **54**, 072003 (2014).
[9] A. Mollén, I. Pusztai, et al, *Phys. Plasmas* **19**, 052307 (2012).
[10] A. Mollén, I. Pusztai, et al, *Phys. Plasmas* **20**, 032310 (2013).

The authors are grateful to J. Candy for providing the GYRO code and E. Belli for the NEO simulations.